A GENUINELY MULTIDISCIPLINARY JOURNAL

CHEMPLUSCHEM

CENTERING ON CHEMISTRY

Accepted Article

Title: Efficient Synthesis of Arylenedioxy-Bridged Porphyrin Dimers through Catalyst-Free Nucleophilic Aromatic Substitution

Authors: Ken-ichi Yamashita, Narumi Kuramochi, Hang Pham Qui Van, Kazuhiro Furutani, Takuji Ogawa, and Ken-ichi Sugiura

To be cited as: *ChemPlusChem* 10.1002/cplu.201900670

Link to VoR: http://dx.doi.org/10.1002/cplu.201900670

A Journal of

ChemPubSoc Europe

WILEY-VCH

www.chempluschem.org

10.1002/cplu.201900670

WILEY-VCH

FULL PAPER

Efficient Synthesis of Arylenedioxy-Bridged Porphyrin Dimers through Catalyst-Free Nucleophilic Aromatic Substitution

Ken-ichi Yamashita,*[a,b] Narumi Kuramochi,[a] Hang Pham Qui Van,[a] Kazuhiro Furutani,[b] Takuji Ogawa,[b] and Ken-ichi Sugiura*[a]

Abstract: A series of porphyrin dimers bridged by one or two rigid arylenedioxy linkers was successfully synthesized by catalyst-free *meso*-aryloxylation involving nucleophilic aromatic substitution. The orientational freedom and conformation of the two porphyrin macrocycles in the mono-bridged dimers depended on the steric hindrance between the macrocycles and substituents on the arylenedioxy linkers. On the other hand, the bis-bridged dimers exhibited a highly rigid cofacial conformation with a distinct interplanar distance. The fluorescence quantum yields of the bis-bridged dimers (Φ_{fl} = 0.094 and 0.096) were quite similar to those of the monomers (Φ_{fl} = 0.13). Owing to their high rigidities, the nonradiative deactivation of the photoexcited states associated with dimerization, which are observed for reported dimers, are mostly suppressed, suggesting that those dimers have highest rigidities among the cofacial porphyrin dimers exploring emission properties. Cyclic voltammetry revealed the electronic communication between the porphyrin macrocycles in the closely stacked bis-bridged dimer.

Introduction

Cofacial porphyrin dimers, whose porphyrin units are bridged by one or more linker units, have attracted considerable attention owing to their unique potentials, which depend on the orientation of the porphyrin units and, especially, the interplanar distance.[1] For example, closely stacked dimers have been used as artificial reaction centers in a photosystem,[2] the synthetic analogs of diheme centers,[3,4] or catalysts for the activation of small molecules, such as H_2, O_2, or N_2.[5] On the other hand, a dimer with a considerably large cavity surrounded by two porphyrin macrocycles can bind guest molecules or anions of suitable molecular size in the cavity through axial coordination to the metal center and/or π-π or CH-π interaction.[6] Such functions are greatly affected by not only the orientation of the two porphyrin macrocycles, but also their orientational flexibility. Flexible dimers can bind guests of various size by changing the orientation of the porphyrin macrocycles.[7] This orientational change has been occasionally applied to amplify the circular dichroism signals of chiral guest molecules during the determination of their chirality.[6,8] On the other hand, orientational rigidity is typically increased to enhance the size selectivity of the dimers for guest molecules.

To date, although various synthetic methods have been reported, the exploration of cofacial porphyrin dimers, especially closely stacked rigid dimers, remains challenging. Their syntheses typically require complicated multi-step reactions that result in low total yields for porphyrin formation[2d,9] or palladium-catalyzed coupling reactions.[2f,2g,10] Recently, dimers have been effectively prepared through self-assembly driven by labile coordination or hydrogen bonding.[11] However, the lability of the bonding causes structural instability upon environmental change.

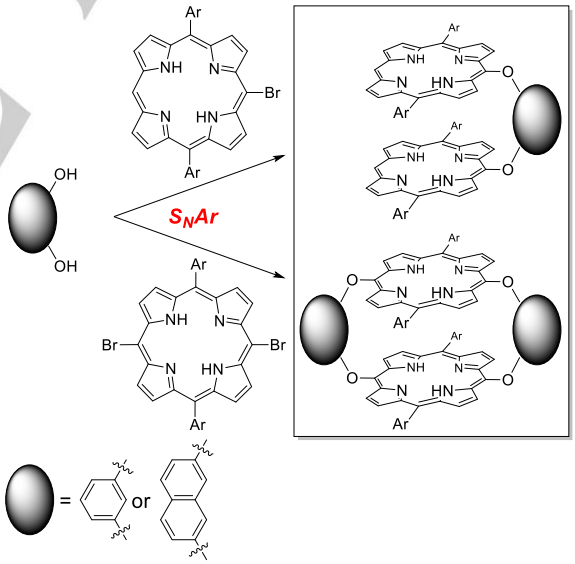

Scheme 1. Schematically representing the construction of arylenedioxy-bridged porphyrin dimers in this work.

Our group[12] and others[13] have recently developed facile synthetic methods for the preparation of *meso*-functionalized porphyrins (e.g., *meso*-aryloxyporphyrins) via the catalyst-free nucleophilic aromatic substitution (S_NAr) of *meso*-halo- or *meso*-nitroporphyrins. These methods do not require expensive or unstable reagents, and the starting materials, i.e., *meso*-bromoporphyrins, are readily available.[14] Moreover, the product

[a] Dr. K. Yamashita, N. Kuramochi, H. Pham Qui Van, Prof. Dr. K. Sugiura
Department of Chemistry, Graduate School of Science and Engineering
Tokyo Metropolitan University
1-1 Minami-Osawa, Hachioji, Tokyo 192-0397 (Japan)
E-mail: yamashita-k@chem.sci.osaka-u.ac.jp, sugiura@porphyrin.jp
[b] Dr. K. Yamashita, K. Furutani, Prof. Dr. T. Ogawa
Department of Chemistry, Graduate School of Science
Osaka University
1-1 Machikaneyama, Toyonaka, Osaka 560-0043 (Japan)

Supporting information for this article is given via a link at the end of the document.

yields are typically quite high. Herein, we report the application of these reactions to the facile synthesis of various covalently bridged porphyrin dimers, especially cofacial dimers. As described below, dihydroxyarenes, such as resorcinols (i.e., 1,3-hydroxyphenols) or 2,7-dihydroxynaphthalene, were adopted as the nucleophiles and, consequently, the linker units in the dimer (Scheme 1).

Results and Discussion

Molecular design

One of the important targets of this study is the synthesis of a rigid cofacial porphyrin dimer. Considering their ready availability and handling ease, dihydroxyarenes were selected as the nucleophiles in the developed S_NAr reactions to produce arylenedioxy-bridged porphyrin dimers (Scheme 1). To realize a nearly cofacial conformation for the two porphyrin macrocycles without structural strain, 1,3-phenylenedioxy or 2,7-naphthylenedioxy linker was adopted among a series of arylenedioxy linkers (Figure 1). The orientations of the two porphyrin macrocycles are expected to be affected by both the number of linker units in the structure and the neighboring substituents on the resorcinol. For mono-bridged dimers, three types of conformation are expected: open (A), intermediate (B), and cofacial (C) (Scheme 2). If there are neighboring substituents on the resorcinol (R^2 and R^3), the conformation is expected to be regulated because of steric repulsion between the porphyrin macrocycles and substituents. A rigid cofacial mono-bridged dimer can be obtained using a 4,6-substituted resorcinol as the nucleophile. Undoubtedly, the introduction of two or more linkers into the dimer is expected to produce a more rigid cofacial structure regardless of the presence of neighboring substituents on the resorcinol. The interplanar distance between the two porphyrin macrocycles is determined by the core arene (i.e., the O···O distance in the linker unit).

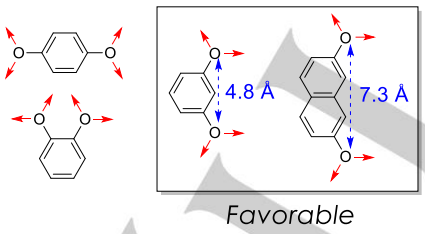

Figure 1. Selection of favorable arylenedioxy linker units for cofacial porphyrin dimers. The red arrows indicate possible porphyrin macrocycle directions.

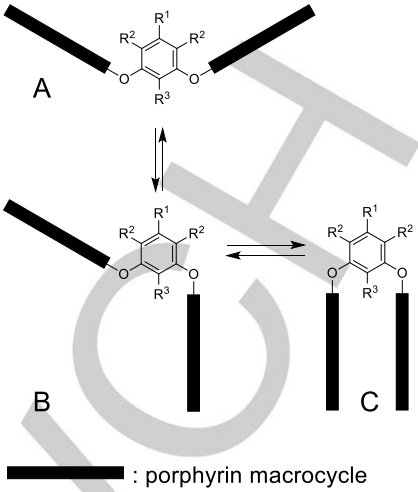

Scheme 2. Equilibrium among the three possible conformations of the mono-bridged dimers, namely, open (A), intermediate (B), and cofacial (C).

Synthesis of monoarylenedioxy-bridged porphyrin dimers

Initially, we investigated the synthesis of monoarylenedioxy-bridged porphyrin dimers **1a–e** by the S_NAr reaction of *meso*-bromodiarylporphyrin **2** with the corresponding resorcinol derivatives **3a–e**. Typically, 4 equivalents of **2** were treated with **3** and a base (K_2CO_3 or K_3PO_4) in refluxing butyronitrile (^{n}PrCN). Except for **1c** and **1e**, the desired dimers were obtained in good yields (69–84%, Table 1). The reactions of 4,6-diethylresorcinol (**3c**) and 2-methylresolcinol (**3d**) were slower than those of the others because of steric hindrance (entries 3 and 5). Their reaction times were improved using K_3PO_4 instead of K_2CO_3 (entries 4 and 6). The reaction of **3e** did not afford any products because of the larger steric hindrance posed by the 2-acetyl group (entry 7). Similarly, the reaction of **2** with 2,7-dihydroxynathhthalene (**4**) gave dimer **5** in 72% yield (entry 8).

Notably, reacting **3b–d** in *N,N*-dimethylformamide (DMF) or *N,N*-dimethylacetamide (DMA), which were used as solvents in a previous study,[12d] resulted in significantly lower yields of **1b–d**, along with the formation of the debrominated by-product of **2**. These side reactions were not observed during the reaction of acetyl-substituted resorcinols **3a** and **3e**. Therefore, debromination results from the electron transfer reaction of **2** with electron-rich nucleophiles, which was also observed in a previous study.[12d]

Table 1. Synthesis of monoarylenedioxy-bridged porphyrin dimers.[a]

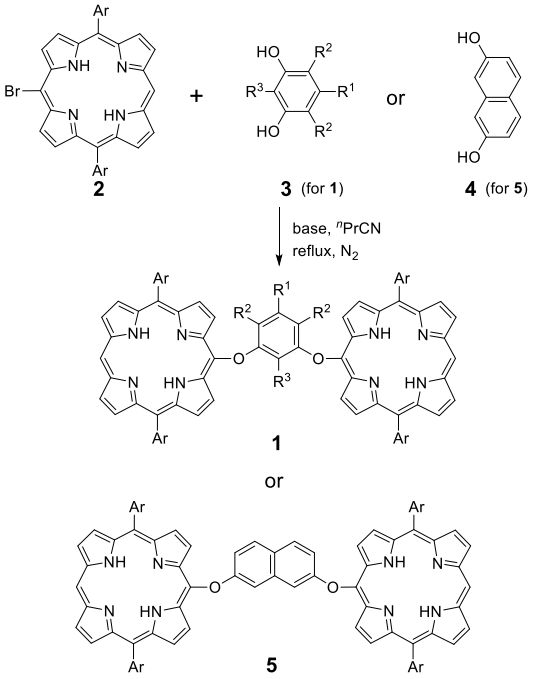

a: R^1 = Ac, R^2 = R^3 = H
b: R^1 = R^2 = R^3 = H
c: R^1 = R^3 = H, R^2 = Et
d: R^1 = R^2 = H, R^3 = Me
e: R^1 = R^2 = H, R^3 = Ac

Entry	**3** or **4**	Base	Time (h)	Product	Yield (%)[b]
1	**3a**	K_2CO_3	21	**1a**	81
2	**3b**	K_2CO_3	25	**1b**	84
3[c]	**3c**	K_2CO_3	94	**1c**	37[d]
4	**3c**	K_3PO_3	22.5	**1c**	19[d]
5	**3d**	K_2CO_3	46	**1d**	69
6	**3d**	K_3PO_4	6	**1d**	71
7	**3e**	K_2CO_3	24	**1e**	0[d]
8	**4**	K_2CO_3	24	**5**	72

[a] Reaction conditions: **2**, 0.080 mmol; **3** or **4**, 0.020 mmol; base, 0.10 mmol; ^{n}PrCN 2 mL; refluxed under N_2. [b] Isolated yield. [c] 3 equiv. of **2**, and 20 equiv. of K_2CO_3 was used. [d] Debrominated byproduct was also formed. [d] No products were afforded.

Synthesis of bis(arylenedioxy)-bridged cyclic porphyrin dimers

There have been quite limited reports on syntheses of the closely-stacked bis-bridged dimers with covalent linker, and they provide low yield of products or require high-dilution condition in the cyclization step.[9a, 9c] Therefore, we investigated the S_NAr reaction of *meso*-dibromodiarylporphyrin **6** with resorcinol **3b** or 2,7-dihydroxynaphthalene (**4**) to produce cyclic porphyrin dimer **7** or **8**, respectively (Scheme 3). Both dimers were obtained in considerably high yields (61% and 69% for **7** and **8**, respectively) under the optimized conditions. Notably, their syntheses did not require highly dilute condition ([**6**] was ca. 5–6 mM).

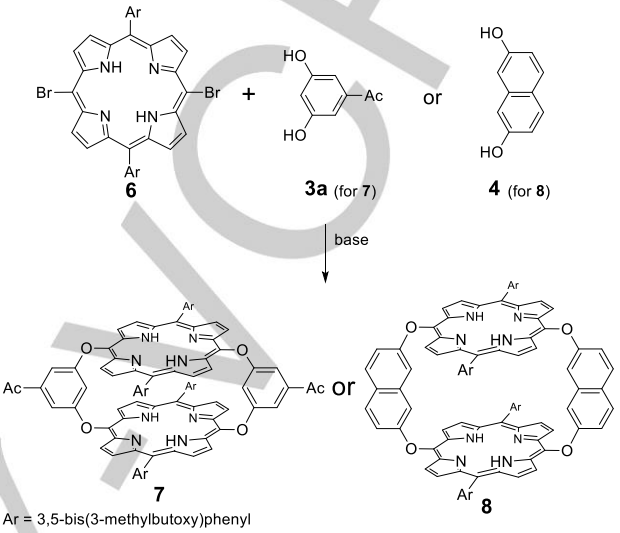

Scheme 3. Synthesis of bis(arylenedioxy)-bridged cyclic porphyrin dimers **7** and **8**.

X-ray crystallography

To gain information on the conformations of the prepared dimers in the solid state, we attempted to produce single crystals for X-ray diffractometry. Among the mono-bridged dimers, only **1b** and **5** afforded suitable single crystals. Although these structures were not able to be solved completely due to poor diffraction data, the preliminary structures (Figure S3) reveal that both **1b** and **5** adopt conformation B (Scheme 2) in the solid state. The distances between the two porphyrin centers of **1b** and **5** are 11.1 and 13.3 Å, respectively.

The successful X-ray diffraction studies of bis-bridged dimers **7** and **8** unambiguously confirm the adoption of the cofacial conformation in the solid state (Figure 2). As expected, the two porphyrin macrocycles are almost parallel with small planar angles [1.31(4)° and 0.00(3)° for **7** and **8**, respectively]. The distances between the centers of the porphyrin macrocycles of **7** and **8** are 4.759 and 7.541 Å, respectively. These distances are quite similar to those between the two oxygen atoms in the arylenedioxy linkers (ca. 4.84 and 7.30 Å for **7** and **8**, respectively). The planar angle between each porphyrin macrocycle and the phenyl ring in the arylenedioxy linker units range between 76.4° and 79.7° for **7** and 88.2° for **8**. These orthogonal orientations are due to steric repulsion between the β-protons on the porphyrin macrocycles and the protons on the arylenedioxy linkers. Thus, the interplanar distance and size of the internal cavity are mostly determined by the length of the arylenedioxy linker, as we expected.

There are no residual electron density peaks within the cavity of **7** (volume: 109 Å^3), confirming its emptiness (Figure S6a,b). On the other hand, **8** has larger cavity (volume: 274 Å^3). Within the cavity, residual electron density peaks derived from the severely disordered solvent molecules (probably THF) are found (Figure S8c,d). This suggests the guest-inclusion ability of **8**.

The porphyrin planes in both crystals **7** and **8** are oriented in almost the same direction (Figure 3). Furthermore, the molecules of **8** are arranged in π-stacked columns.

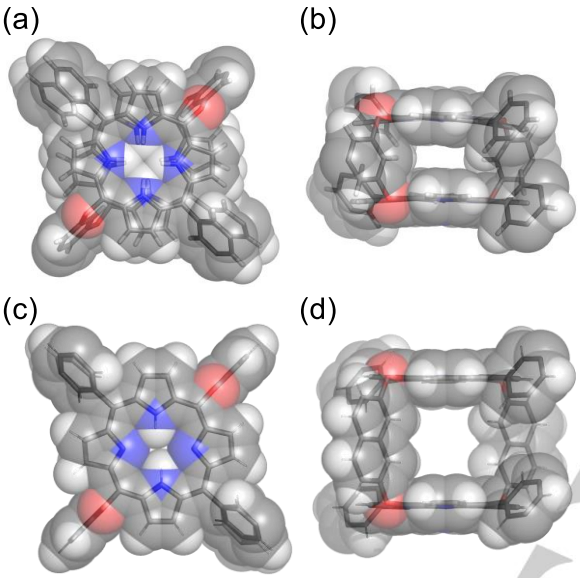

Figure 2. (a, c) Top and (b, d) side views of the crystal structures of **7** and **8**, respectively (C = gray, H = white, N = blue, and O = red). Substituents on the aryl groups and solvent molecules are omitted for clarity. The two inner NH protons of each porphyrin macrocycle of **7** were statistically disordered over the four N atoms.

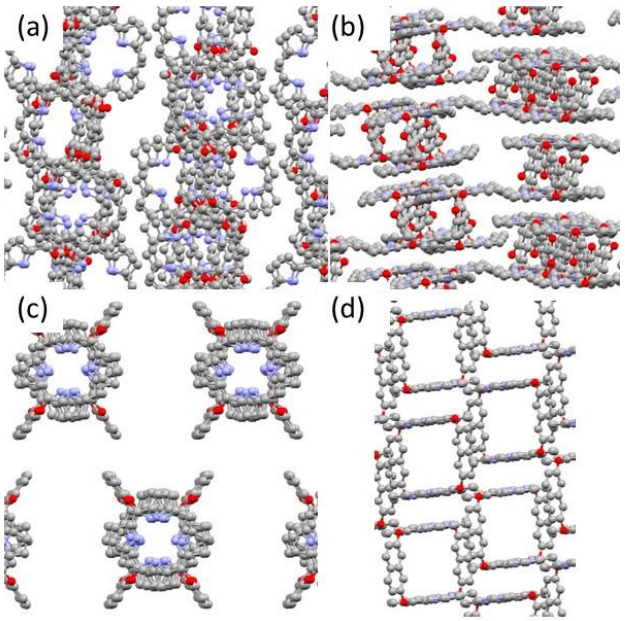

Figure 3. Packing structures of (a, b) 7 and (c, d) 8. (C = gray, N = blue, and O = red). The aryl groups, hydrogen atoms, and solvent molecules are omitted for clarity.

Conformational analysis of the dimers by ^{1}H NMR spectroscopy

The orientations of the two porphyrin macrocycles of the prepared dimers in solution were analyzed by ^{1}H NMR spectroscopy. As discussed above, this orientation is expected to be regulated by the neighboring substituents on the arylenedioxy linker (R^2 and R^3) of mono-bridged dimer **1**. The conformational differences are reflected in the ^{1}H NMR spectra of dimers **1a–d** (Table 2, Figures S1 and S2). The chemical shifts of the porphyrin proton signals (H_{meso}, H_β, and inner N*H*) of **1a** and **1b** are quite similar to those of monomer **9** (Figure 4),[12d] confirming the high conformational freedom of **1a** and **1b**.

On the other hand, the chemical shifts of the porphyrin proton signals of **1c** are considerably upfield relative to those of the other compounds; for example, the δ(N*H*) values of **1c** and **9**, are −3.82 and −2.77 ppm ($\Delta\delta$ = −1.05 ppm), respectively. In addition, the singlet signal of the proton on position 2 of the phenylenedioxy linker (H_{L1}) of **1c**, observed at 5.59 ppm, is considerably upfield shifted. These upfield shifts are characteristic of a cofacial conformation and are attributed to the shielding effect caused by aromatic ring current interactions between the closely associated porphyrin macrocycles. Moreover, the proton signals of the two ortho protons and two alkoxy substituents in the Ar groups of **1c** are broadened and/or inequivalently observed (Figure 5b). These results also indicate a cofacial conformation for **1c** because the split peaks are assignable to endo and exo protons on the basis of the roughly orthogonal orientations of the aryl rings and porphyrin macrocycles (Figure 5e) and the rotational-motion restriction of the aryl rings at room temperature on the NMR timescale due to steric hindrance. The chemical shifts of the porphyrin proton signals of **1d** are slightly downfield relative to

those of **1a** and **1b**. Moreover, compared to the chemical shifts of 2-methyl-1,3-dimethoxybenzene,[15] the signal for the L2 proton is upfield shifted ($\Delta\delta$ = −0.84 ppm) while that of the methyl protons on the linker units is considerably downfield shifted ($\Delta\delta$ = −1.74 ppm). These shifts are the result of the diatropic ring current associated with the 18π aromatic porphyrin macrocycle, and suggests that **1d** has a fixed open conformation (A).

Understandably, bis-bridged dimers **7** and **8** are strictly fixed in a cofacial conformation. The chemical shifts of the porphyrin proton signals of **7** and **8** are upfield relative to those of the corresponding monomer (i.e., **10**) and mono-bridged dimers (i.e., **1** and **5** for **7** and **8**, respectively). Moreover, the degree of the shift for **7** is larger than that for **8**; for example, the δ(N*H*) values of **7** and **8** are −4.25 and −3.10 ppm, respectively, which reflects the difference in the interplanar distances revealed by the crystallographic studies. As was observed for **1c**, the signals for the two ortho protons and the two alkoxy substituents in the Ar groups of **7** and **8** are observed to be completely inequivalent (Figure 5c,d). This reflects the completely fixed cofacial conformations of the bis-bridged dimers, in contrast to the certain amount of conformational freedom observed for the mono-bridged cofacial dimer **1c**.

Table 2. Selected ^{1}H NMR data for the prepared compounds (500 MHz, $CDCl_3$).

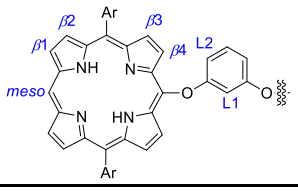

	δ / ppm							
	H_{meso}	$H_{\beta4}$	$H_{\beta1}$	$H_{\beta2}$	$H_{\beta3}$	H_{L1}	H_{L2}	N*H*
1a	10.14	9.38	9.29	9.12	9.06	7.59	6.92	−2.80
1b	10.12	9.46	9.28	9.11	9.06	7.54	6.31	−2.78
1c	9.59	8.95	8.88	8.73	8.56	5.59	-[b]	−3.82
1d	10.12	9.58	9.29	9.12	9.10	-[b]	5.74	−2.72
5	10.03	9.24	9.20	9.02	8.86	7.32	6.64	−2.94
9[a]	10.10	9.38	9.26	9.10	8.98	-[b]	-[b]	−2.77
7	-[b]	8.77	=[c]	=[d]	8.53	4.00	8.16	−4.25
8	-[b]	8.94	=[c]	=[d]	8.58	4.54	7.92	−3.10
10[a]	-[b]	9.29	=[c]	=[d]	8.90	-[b]	-[b]	−2.49

[a] Data from ref. 12d. [b] No proton available. [c] Equivalent to $H_{\beta4}$. [d] Equivalent to $H_{\beta3}$.

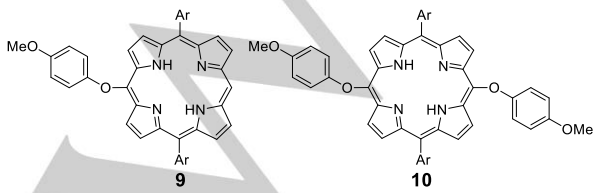

Figure 4. Chemical structures of the reference monomers.[12d]

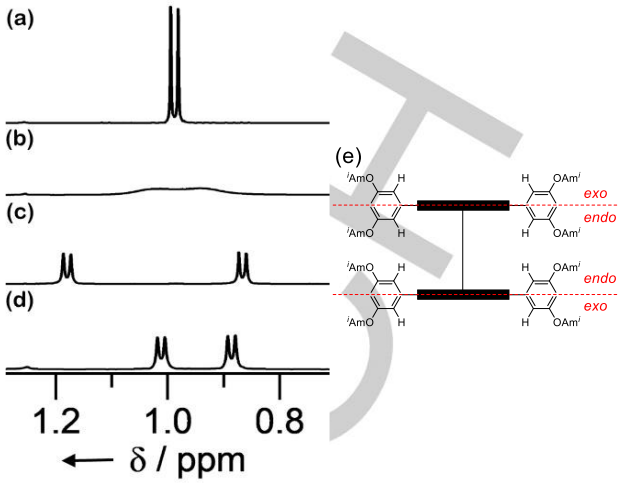

Figure 5. Partial ^{1}H NMR spectra of (a) **1a**, (b) **1c**, (c) **7**, and (d) **8** representing the terminal methyl signals of the OAm^i (3-methylbutoxy) substituents (500 MHz, $CDCl_3$). (e) Schematic representation of the regiochemistry of the aryl proton of the cofacial porphyrin dimers (**1c**, **7**, and **8**).

Spectroscopic comparison

Solution-conformation information was also obtained by UV/vis absorption studies. The Soret band region of the spectra is shown in Figure 6, with the entire spectra shown in Figures S9 and S10. Among the mono-bridged dimers, **1c** exhibits the largest blue-shift of the Soret band (414 nm) with respect to that of reference monomer **9** (417 nm[12d]). In addition, its Soret band is significantly broadened. These spectroscopic features are characteristic of cofacial porphyrin dimers and can be explained well by exciton coupling.[16] Therefore, these results, as well as those of the ^{1}H NMR study, strongly indicate that **1c** adopts a cofacial conformation in solution.

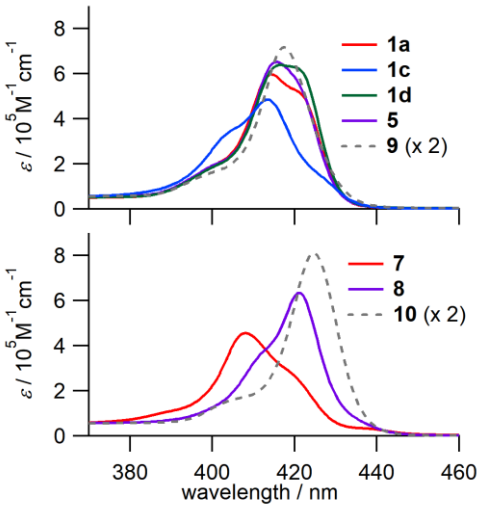

Figure 6. Soret bands in the UV/vis absorption spectra of the prepared compounds in toluene. The extinction coefficients of monomers **9** and **10** have been doubled.

The Soret bands of both bis-bridged dimers are considerably blue-shifted, with **7** exhibiting the greatest shift. This suggests that the structures of the bis-bridged dimers obtained by X-ray diffractometry are essentially retained, even in solution. Dimerization was found to have quite a small effect on the positions of the longest wavelength bands, which are determined only by the number of *meso* substituents.

Fluorescence data for **1a**, **7**, **8**, **9**, and **10** are summarized in Table 3, and the spectra are shown in Figure S11. As was observed for the positions of the longest-wavelength UV/vis absorption bands, the positions of the emission peaks and spectral shapes are primarily determined by the number of *meso* substituents. The fluorescence quantum yields (Φ_{fl}) of both mono- and bis-bridged dimers are slightly lower than those of the reference monomers. Notably, the dependence of the interplanar distance on the spectral shape and Φ_{fl} is very small based on the data for **7** and **8**. This small dependence is uncommon because the reported cofacial dimers, mainly mono-bridged dimers, have considerably low Φ_{fl} values with strong distance-dependence;[2a-d,5d,9d] for example, the Φ_{fl} values of a mono-anthracene- and biphenylene-bridged dimers are 0.22 and 0.04, respectively, relative to the corresponding monomer.[2c,2d] The decrease in Φ_{fl} due to dimerization have been explained by the strong π-orbital overlap in face-to-face dimers leading to non-fluorescence decay processes.[2a,2b] However, our results do not fit this explanation; instead, we suggest that π-orbital overlap is not the main factor governing the decrease in Φ_{fl}. The major difference between the previously reported dimer and the dimer reported herein lies in structural rigidities; i.e., various intramolecular motions, such as slipping and pacman-like motion, are structurally allowed in mono-bridged dimers bridged even by rigid linkers, while those, especially the pacman-like motion, are significantly hindered in our dimers. The high structural rigidities of the bis-bridged dimers prevent the nonradiative deactivation associated with dimerization. These observations suggest that **7** and **8** have the highest rigidities among the cofacial porphyrin dimers exploring emission properties.

Table 3. Fluorescence data for the prepared compounds in toluene excited at 520 nm.

	λ_{fl} / nm[a]	Φ_{fl}[b]
1a	648, 714	0.077 (0.93)
9	649, 715	0.083
7	664, 735	0.094 (0.72)
8	663, 733	0.096 (0.74)
10	664, 733	0.130

[a] Wavelengths of the emission maxima. [b] Fluorescence quantum yield. The values in parentheses are relative ones to the corresponding monomers.

Electrochemistry

To obtain further insight into the electronic communication between the two porphyrin macrocycles of the dimers, **1a**, **7**, and **8** were subjected to cyclic voltammetry. The effect of stacking was clearly observed in the reduction events. The oxidation and reduction potentials of **1a**, **7**, **8**, as well as those of previously reported **9** and **10**, are summarized in Table S2, with the cyclic voltammograms of **1a**, **7**, and **8** shown in Figure 7. The potentials of the dimers are almost the same as those of the reference monomers. It is noteworthy that the first reduction wave of **7** is split (−1.64 and −1.74 V vs. Fc/Fc^+) and the second reduction wave is irreversible, which indicates that the two porphyrin moieties in **7** are reduced in a stepwise manner due to the electronic communication between them. On the other hand, no splitting is observed for the first reduction wave of **8**, rather its second reduction wave is split, which indicates that electronic communication between the more separated porphyrin moieties in **8** is weaker than that in **7**, but is not negligible.

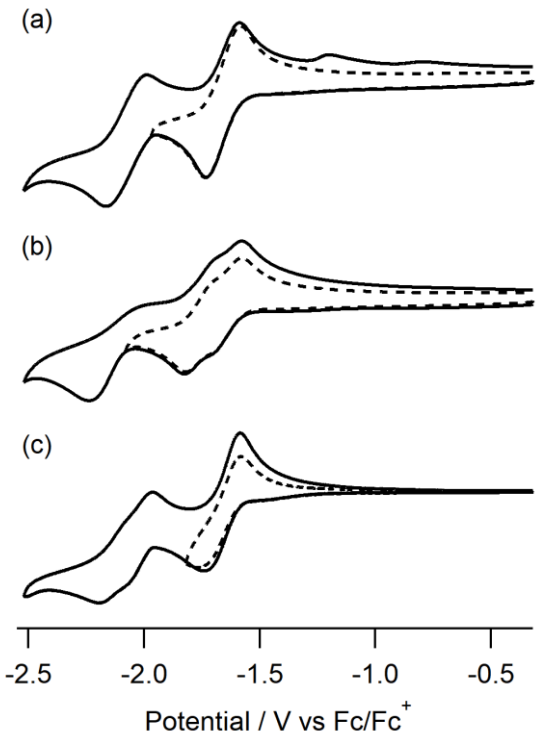

Figure 7. Cyclic voltammograms of (a) **1a**, (b) **7**, and (c) **8** in CH_2Cl_2 containing 0.1 M $TBAPF_6$.

Conclusions

We have reported a practical and efficient procedure for the synthesis of arylenedioxy-bridged porphyrin dimers via catalyst-free nucleophilic substitution. In most cases, the product yields were considerably high. The orientations of the two porphyrin macrocycles and degree of orientational freedom are controlled by both the number of linker units in the structure and the neighboring substituents on the resorcinol. In particular, the highly rigid cofacial structures of the bis-bridged dimers were revealed by X-ray diffraction and spectroscopic studies. Owing to the high rigidities of the bis-bridged dimers, the nonradiative deactivation of the photoexcited states associated with dimerization, which are

typically observed for reported dimers, are mostly suppressed, suggesting that **7** and **8** have highest rigidities among the cofacial porphyrin dimers exploring emission properties. For the closely stacked bis-bridged dimer, electronic communication between the porphyrin macrocycles was observed in the electrochemical study. The small dimer **7** has a small empty cavity while the larger dimer **8** has a cavity that can encapsulate small molecules. Our preliminary experiments suggest that several linear alkane molecules can be encapsulated within the cavity of **8**. We anticipate that the synthesis method developed herein will contribute to the further development of the chemistry of cofacial porphyrin dimers. We also anticipate that these bis-bridged dimers are some of the most rigid dimers reported to date, and thus exhibit significant selectivities and/or affinities during molecular recognition or catalysis. We are currently developing this chemistry, the results of which will be reported in due course.

Experimental Section

Instrumentation and Materials

5-Bromo-10,20-bis[3,5-bis(3-methylbutoxy)phenyl]porphyrin (**2**)[17] 5,15-dibromo-10,20-bis[3,5-bis(3-methylbutoxy)phenyl]porphyrin (**6**)[17b], and the reference monomers (**9** and **10**)[12d] were synthesized by previously reported procedures. *N,N*-Dimethylformamide (DMF), *N,N*-dimethylacetamide (DMA), butyronitrile (^{n}PrCN), and toluene were distilled from CaH_2. All other chemicals were of reagent grade and used without any further purification. $CDCl_3$ was acquired from Acros Organics. Analytical thin layer chromatography (TLC) was performed on silica gel 60 F_{254} plates. Flash column chromatography was performed using silica gel 60N (spherical, neutral, 40–50 μm). All NMR spectral data were recorded on a 500 MHz spectrometer at ambient temperature (25 °C) unless otherwise noted. ^{1}H NMR spectra were referenced internally to tetramethylsilane as the standard. ^{13}C NMR spectra were referenced internally to solvent signals (δ = 77.0 ppm for $CDCl_3$). APCI HRMS data were measured on a Bruker micrOTOF II equipped with the DirectProbe assembly. ESI HRMS data were measured on a Bruker micrOTOF QIII. IR spectral data were recorded on a PerkinElmer Spectrum Two spectrometer equipped with an ATR unit. UV/vis spectral data were recorded on Shimadzu UV-3600 or UV-3150 spectrometers. Fluorescence spectral data were recorded on a JASCO FP-8200 fluorescence spectrometer. Measurements were performed without deaeration of the sample solution. The fluorescence quantum yields were estimated by taking tetraphenylporphyrin in toluene as the standard (Φ_f = 0.11).[18] Melting points were determined on a Yanaco MP-S3 melting point apparatus. Cyclic voltammetry (CV) measurements were carried out using ALS 650C electrochemical analyzer in argon-saturated CH_2Cl_2 solutions containing 0.1 M tetrabutylammonium hexafluorophosphate as a supporting electrolyte at ambient temperature (298 K). A conventional three-electrode cell was used with a glassy carbon working electrode, a platinum wire counter electrode, and an Ag/AgCl reference electrode. Ferrocene was used as the internal standard in all electrochemical experiments.

Synthesis of 4,6-diethylresorcinol (3c)[19]

This compound was synthesized in a similar manner to the synthesis of the related compounds.[20] To a suspension of 4,6-diacetylresorcinol (1.942 g, 10 mmol) and Zn powder (13.078 g, 200 mmol) in ethanol (200 mL) at 0 °C, concentrated hydrochloric acid (50 mL) was added dropwise. The resultant mixture was stirred at room temperature for 1.5 hours. The unreacted zinc powder was removed by filtration, and the filtrate was diluted with water (300 mL). The product was extracted with Et_2O. The organic layer was washed with aqueous $NaHCO_3$ and brine, and dried over $MgSO_4$. Solvent was removed under the reduced pressure. The crude product was purified by flash column chromatography (silica gel, toluene/EtOAc = 10:1, then 5:1) to give **3c** as a pink waxy solid (1.181 g, 7.11 mmol, 71%). ^{1}H NMR data were consistent with the previously reported one.[19] ^{1}H NMR (500 MHz, $CDCl_3$) δ = 6.85 (s, 1H), 6.28 (s, 1H), 4.98 (brs, 2H), 2.54 (q, *J* = 7.6 Hz, 4H), 1.19 ppm (t, *J* = 7.6 Hz, 6H).

General procedure for the synthesis of 1,3-phenylenedioxy-bridged porphyrin dimer 1

5-Bromo-10,20-bis[3,5-bis(3-methylbutoxy)phenyl]porphyrin (**2**) (0.080 mmol), resorcinol derivative **3** (0.020 mmol), and K_2CO_3 (0.10 mmol) were mixed in dry butyronitrile (2 mL). The mixture was purged with N_2 and refluxed with stirring while protected against exposure to light. The reaction was monitored by TLC. After the reaction was complete, the reaction mixture was filtrated to remove K_2CO_3, and then solvent was evaporated under reduced pressure. The crude product was purified by flash column chromatography (silica gel) to give **1**.

Mono-(5-acetyl-1,3-phenylenedioxy)-bridged porphyrin dimer 1a

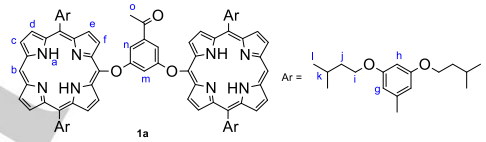

2 was reacted with 5-acetylresorcinol (**3a**) for 21 h according to the general procedure. The crude product was purified by flash column chromatography (silica gel, hexane/toluene 1:2) to give **1a** as a purple solid (81%). Analytically pure sample was obtained by recrystallization from hot toluene/hexane as a purple powder. R_f = 0.55 (toluene); m.p. 280−281 °C; ^{1}H NMR (500 MHz, $CDCl_3$) δ = 10.14 (s, 2H, H_b), 9.38 (d, *J* = 4.7 Hz, 4H, H_f), 9.29 (d, *J* = 4.7 Hz, 4H, H_c), 9.12 (d, *J* = 4.6 Hz, 4H, H_d), 9.06 (d, *J* = 4.7 Hz, 4H, H_e), 7.59 (t, *J* = 2.3 Hz, 1H, H_m), 7.40 (d, *J* = 2.2 Hz, 8H, H_g), 7.01 (d, *J* = 2.4 Hz, 2H, H_n), 6.92 (t, *J* = 2.2 Hz, 4H, H_h), 4.18 (t, *J* = 6.7 Hz, 16H, H_i), 1.90 (m, *J* = 6.6 Hz, 8H, H_k), 1.82 (s, 3H, H_o), 1.80 (q, *J* = 6.7 Hz, 16H, H_j), 0.99 (d, *J* = 6.6 Hz, 48H, H_l), −2.80 ppm (s, 4H, H_a); ^{13}C NMR (125 MHz, $CDCl_3$) δ = 196.9 (*C*q), 167.0 (*C*q), 158.6 (*C*q), 147.2 (*C*q), 146.7 (*C*q), 146.4 (*C*q), 142.9 (*C*q), 141.7 (*C*q), 139.6 (*C*q), 131.7 (*C*H), 131.5 (*C*H), 131.3 (*C*q), 131.2 (*C*H), 127.4 (*C*H), 119.8 (*C*q), 114.5 (*C*H), 109.7 (2×*C*H), 104.8 (*C*H), 101.1 (*C*H), 66.8 (CH_2), 38.1 (CH_2), 26.5 (CH_3), 25.1 (*C*H), 22.7 ppm (CH_3); IR (ATR): $\tilde{\nu}$ = 3297, 2954, 2928, 2869, 1690, 1587, 1430, 1406, 1331, 1291, 1152, 1055, 923, 848, 791, 727, 691 cm^{-1}; UV/Vis (toluene): λ_{max} (Logε) = 415 (5.78), 510 (4.58), 544 (4.08), 586 (4.02), 643 nm (3.73); HRMS(APCI): *m/z* calcd for $C_{112}H_{129}N_8O_{11}$: 1762.9808 ([*M*+H]$^+$); found 1762.9792; elemental analysis calcd (%) for $C_{112}H_{128}N_8O_{11}$: C, 76.33; H, 7.32; N, 6.36; found: C, 76.06; H, 7.30; N, 6.18.

Mono-(1,3-phenylenedioxy)-bridged porphyrin dimer 1b

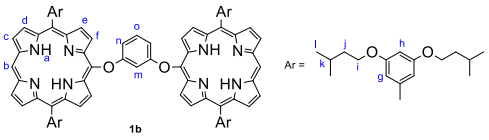

2 was reacted with resorcinol (**3b**) for 25 h according to the general procedure. The crude product was purified by flash column chromatography (silica gel, hexane/toluene 1:1, then 1:1.5) to give **1b** as

a purple solid (84%). Analytically pure sample was obtained by recrystallization from hot octane as a purple powder. R_f = 0.15 (hexane/toluene 1:1); m.p.: 263−264 °C; ^{1}H NMR (500 MHz, $CDCl_3$) δ = 10.12 (s, 2H, H_b), 9.46 (d, J = 4.8 Hz, 4H, H_f), 9.28 (d, J = 4.7 Hz, 4H, H_c), 9.11 (d, J = 4.6 Hz, 4H, H_d), 9.06 (d, J = 4.7 Hz, 4H, H_e), 7.54 (t, J = 2.4 Hz, 1H, H_m), 7.40 (d, J = 2.2 Hz, 8H, H_g), 6.91 (t, J = 2.2 Hz, 4H, H_h), 6.81 (t, J = 8.5 Hz, 1H, H_o), 6.31 (dd, J = 6.1 and 2.3 Hz, 2H, H_n), 4.18 (t, J = 6.7 Hz, 16H, H_i), 1.90 (m, J = 6.7 Hz, 8H, H_k), 1.81 (q, J = 6.8 Hz, 16H, H_j), 1.00 (d, J = 6.7 Hz, 48H, H_l), −2.78 ppm (s, 4H, H_a); ^{13}C NMR (125 MHz, $CDCl_3$) δ = 167.2 (*C*q), 158.6 (*C*q), 147.1 (*C*q), 146.6 (*C*q), 146.3 (*C*q), 143.0 (*C*q), 142.1 (*C*q), 132.0 (*C*q), 131.7 (*C*H), 131.4 (*C*H), 131.1 (*C*H), 130.0 (*C*H), 127.8 (*C*H), 119.7 (*C*q), 114.5 (*C*H), 110.2 (*C*H), 105.6 (*C*H), 104.6 (*C*H), 101.1 (*C*H), 66.8 (CH_2), 38.2 (CH_2), 25.1 (*C*H), 22.7 ppm (CH_3); IR (ATR): $\tilde{\nu}$ = 3294, 2954, 2926, 2869, 1588, 1429, 1332, 1245, 1158, 1130, 1062, 965, 924, 848, 794, 780, 732, 691 cm^{-1}; UV/Vis (toluene): λ_{max} (Logε) = 415 (5.79), 510 (4.59), 544 (4.10), 586 (4.02), 643 nm (3.75); HRMS(APCI): *m/z* calcd for $C_{110}H_{127}N_8O_{10}$: 1720.9702 ([M+H]$^+$), found 1720.9647; elemental analysis calcd (%) for $C_{110}H_{126}N_8O_{10}$: C, 76.80; H, 7.38; N, 6.51; found: C, 76.53; H, 7.28; N, 6.30.

Mono-(4,6-diethyl-1,3-phenylenedioxy)-bridged porphyrin dimer 1c

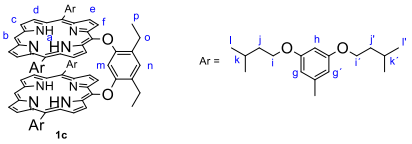

2 was reacted with 4,6-diethylresorcinol (**3c**) for 94 h according to the general procedure, but 3 equiv. of **2** and 20 equiv. of K_2CO_3 was used. The crude product was purified by flash column chromatography (silica gel, hexane/toluene 1:1, then 1:1.5) to give **1c** as a purple solid (37%). Analytically pure sample was obtained by recrystallization from hot octane as a purple powder. R_f = 0.15 (hexane/toluene 1:1); R_f = 0.15 (hexane/toluene 1:1); m.p.: 208−210 °C; ^{1}H NMR (500 MHz, $CDCl_3$) δ = 9.59 (s, 2H, H_b), 8.95 (d, J = 4.7 Hz, 4H, H_f), 8.88 (d, J = 4.5 Hz, 4H, H_c), 8.73 (d, J = 4.5 Hz, 4H, H_d), 8.56 (d, J = 4.7 Hz, 4H, H_e), 7.62 (s, 1H, H_n), 6.96 (brs, 8H, H_g and H_g'), 6.79 (t, J = 2.2 Hz, 4H, H_h), 5.59 (s, 1H, H_m), 4.02 (m, 16H, H_i and H_i'), 3.33 (q, J = 7.4 Hz, 4H, H_o), 2.00–1.68 (m, 30H, H_k, H_j, H_k', H_j' and H_p), 1.02 (brs, 24H, H_l or H_l'), 0.94 (brs, 24H, H_l or H_l'), −3.82 ppm (s, 4H, H_a); ^{13}C NMR (125 MHz, $CDCl_3$) δ = 162.7 (*C*q), 158.4 (*C*q), 142.7 (*C*q), 132.9 (*C*q), 131.1 (*C*H), 130.6 (*C*H), 130.3 (*C*H), 129.8 (*C*H), 126.9 (*C*H), 125.4 (*C*q), 118.8 (*C*q), 114.4 (br, *C*H), 106.8 (*C*H), 103.4 (*C*H), 100.6 (*C*H), 66.6 (CH_2), 38.1 (CH_2), 25.1 (*C*H), 23.6 (CH_2), 22.7 (CH_3), 15.1 ppm (CH_3) (four signals corresponding to the pyrrole α carbons were not observed due to severe exchange broadening through NH tautomerism); IR (ATR): $\tilde{\nu}$ = 3295, 2956, 2928, 2870, 1587, 1464, 1432, 1407, 1383, 1346, 1283, 1243, 1164, 1116, 1056, 965, 923, 846, 833, 789, 729, 689 cm^{-1}; UV/Vis (toluene): λ_{max} (Logε) = 414 (5.69), 513 (4.45), 549 (4.09), 590 (3.90), 647 nm (3.78); HRMS(APCI): *m/z* calcd for $C_{114}H_{135}N_8O_{10}$: 1777.0328 ([M+H]$^+$), found 1777.0289; elemental analysis calcd (%) for $C_{114}H_{134}N_8O_{10}$: C, 77.08; H, 7.60; N, 6.31; found: C, 77.04; H, 7.61; N, 6.13.

Mono-(2-methyl-1,3-phenylenedioxy)-bridged porphyrin dimer 1d

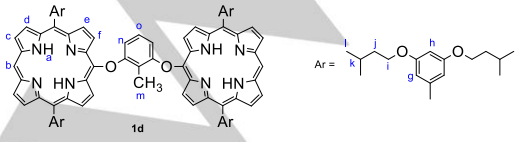

2 was reacted with 2-methylresorcinol (**3d**) for 6 h according to the general procedure, but K_3PO_4 was used instead of K_2CO_3. The crude product was purified by flash column chromatography (silica gel, hexane/toluene 1:1, then 1:1.5) to give **1d** as a purple solid (71%). Analytically pure sample was obtained by recrystallization from hot octane as a purple powder. R_f = 0.28 (hexane/toluene 1:1); m.p.: 162−163 °C; ^{1}H NMR (500 MHz, $CDCl_3$) δ = 10.12 (s, 2H, H_b), 9.58 (d, J = 4.7 Hz, 4H, H_f), 9.29 (d, J = 4.6 Hz, 4H, H_c), 9.12 (d, J = 4.6 Hz, 4H, H_d), 9.10 (d, J = 4.7 Hz, 4H, H_e), 7.41 (d, J = 2.2 Hz, 8H, H_g), 6.93 (t, J = 2.2 Hz, 4H, H_h), 6.20 (t, J = 8.4 Hz, 1H, H_o), 5.74 (d, J = 8.4 Hz, 2H, H_n), 4.20 (t, J = 6.7 Hz, 16H, H_i), 3.86 (s, 3H, H_m), 1.91 (m, J = 6.7 Hz, 8H, H_k), 1.81 (q, J = 6.6 Hz, 16H, H_j), 1.00 (d, J = 6.5 Hz, 48H, H_l), −2.72 ppm (s, 4H, H_a); ^{13}C NMR (125 MHz, $CDCl_3$) δ = 165.4 (*C*q), 158.6 (*C*q), 147.0 (*C*q), 146.6 (*C*q), 146.4 (*C*q), 143.0 (*C*q), 142.2 (*C*q), 132.9 (*C*q), 131.7 (*C*H), 131.4 (*C*H), 131.0 (*C*H), 127.8 (*C*H), 126.2 (*C*H), 119.7 (*C*q), 114.5 (*C*H), 113.8 (*C*q), 110.0 (*C*H), 104.5 (*C*H), 101.1 (*C*H), 66.8 (CH_2), 38.2 (CH_2), 25.1 (*C*H), 22.7 (CH_3), 10.0 ppm (CH_3); IR (ATR): $\tilde{\nu}$ = 3300, 2954, 2923, 2869, 1587, 1461, 1430, 1383, 1336, 1233, 1149, 1117, 1059, 964, 922, 846, 796, 733, 692 cm^{-1}; UV/Vis (toluene): λ_{max} (Logε) = 417 (5.81), 480 (3.85), 510 (4.61), 545 (4.14), 586 (4.04), 643 nm (3.81); MS(APCI): *m/z* calcd for $C_{111}H_{129}N_8O_{10}$: 1733.97 ([M+H]$^+$), found 1733.95; elemental analysis calcd (%) for $C_{111}H_{128}N_8O_{10}$: C, 76.87; H, 7.44; N, 6.46; found: C, 76.61; H, 7.39; N, 6.27.

Mono-(2,7-naphthylenedioxy)-bridged porphyrin dimer 5

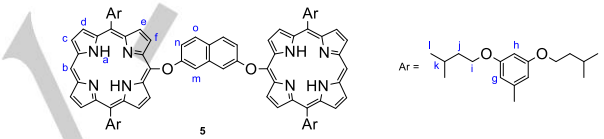

2 was reacted with 2,7-dihydroxynaphthalene (**4**) instead of **3** for 24 h according to the general procedure. The crude product was purified by flash column chromatography (silica gel, hexane/toluene 1:1, then 1:1.5) to give **5** as a purple solid (72%). Analytically pure sample was obtained by recrystallization from hot octane as a purple powder. R_f = 0.33 (hexane/toluene 1:1); m.p.: 270−272 °C; ^{1}H NMR (500 MHz, $CDCl_3$) δ = 10.03 (s, 2H, H_b), 9.24 (d, J = 4.7 Hz, 4H, H_f), 9.20 (d, J = 4.6 Hz, 4H, H_c), 9.02 (d, J = 4.5 Hz, 4H, H_d), 8.86 (d, J = 4.7 Hz, 4H, H_e), 7.76 (d, J = 9.1 Hz, 2H, H_o), 7.32 (dd, J = 7.5, 2.2 Hz, 2H, H_m), 7.27 (d, J = 2.2 Hz, 8H, H_g), 6.85 (t, J = 2.2 Hz, 4H, H_h), 6.64 (d, J = 1.9 Hz, 2H, H_n), 4.12 (t, J = 6.7 Hz, 16H, H_i), 1.86 (m, J = 6.7 Hz, 8H, H_k), 1.76 (q, J = 6.7 Hz, 16H, H_j), 1.00 (d, J = 6.6 Hz, 48H, H_l), −2.94 ppm (s, 4H, H_a); ^{13}C NMR (125 MHz, $CDCl_3$) δ = 164.6 (*C*q), 158.5 (*C*q), 146.9 (*C*q), 146.4 (*C*q), 146.2 (*C*q), 142.8 (*C*q), 141.9 (*C*q), 135.6 (*C*q), 132.0 (*C*q), 131.5 (*C*H), 131.3 (*C*H), 130.9 (*C*H), 129.6 (*C*H), 127.6 (*C*H), 125.1 (*C*q), 119.6 (*C*q), 116.5 (*C*H), 114.4 (*C*H), 111.6 (*C*H), 104.5 (*C*H), 101.0 (*C*H), 66.7 (CH_2), 38.1 (CH_2), 25.1 (*C*H), 22.7 ppm (CH_3); IR (ATR): $\tilde{\nu}$ = 3297, 2954, 2927, 2869, 1588, 1429, 1384, 1336, 1243, 1151, 1057, 965, 922, 845, 833, 792, 725, 691 cm^{-1}; UV/Vis (toluene): λ_{max} (Logε) = 416 (5.81), 510 (4.59), 545 (4.11), 586 (4.02), 643 nm (3.78); HRMS(APCI): *m/z* calcd for $C_{114}H_{129}N_8O_{10}$: 1770.9859 ([M+H]$^+$), found 1770.9839; elemental analysis calcd (%) for $C_{114}H_{128}N_8O_{10}$: C, 77.34; H, 7.29; N, 6.33; found: C, 77.13; H, 7.52; N, 6.19.

Bis-(5-acetyl-1,3-phenylenedioxy)-bridged porphyrin dimer 7

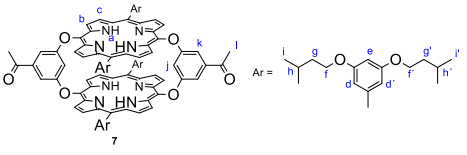

5,15-Dibromo-10,20-bis[3,5-bis(3-methylbutoxy)phenyl]porphyrin (**6**) (200 mg, 0.207 mmol), 5-acetylresolcinol (**3a**) (31.56 mg, 0.207 mmol), and K_2CO_3 (143.27 mg, 1.03 mmol) were mixed in dry DMA (40 mL). The mixture was purged with N_2 and stirred at 120 °C for 5 h while protected

against exposure to light. The reaction mixture was diluted with toluene, washed with water (9 × 50 mL), dried over $MgSO_4$, and concentrated under reduced pressure. The crude product was purified by flash column chromatography (silica gel, toluene, then $CHCl_3$) to give **7** as a purple solid (121.2 mg, 0.063 mmol, 61%). Analytically pure sample was obtained by recrystallization from EtOAc/EtOH as a purple powder. R_f = 0.45 (toluene); m.p.: >300 ºC; ^{1}H NMR (500 MHz, $CDCl_3$) δ = 8.77 (d, J = 4.7 Hz, 8H, H_b), 8.53 (d, J = 4.7 Hz, 8H, H_c), 8.16 (d, J = 2.3 Hz, 4H, H_k), 7.10 (s, 4H, H_d), 6.76 (t, J = 2.2 Hz, 4H, H_e), 6.63 (s, 4H, $H_{d'}$), 4.04 (t, J = 6.9 Hz, 8H, H_f), 4.00 (t, J = 2.3 Hz, 2H, H_j), 3.93 (t, J = 6.7 Hz, 8H, $H_{f'}$), 3.02 (s, 6H, H_l), 2.03 (m, J = 6.7 Hz, 4H, H_h), 1.88 (q, J = 6.9 Hz, 8H, H_g), 1.74 (m, J = 6.7 Hz, 4H, $H_{h'}$), 1.63 (q, J = 6.7 Hz, 8H, $H_{g'}$), 1.18 (d, J = 6.6 Hz, 24H, H_i), 0.87 (d, J = 6.6 Hz, 24H, $H_{i'}$), −4.25 ppm (s, 4H, H_a); ^{13}C NMR (125 MHz, $CDCl_3$) δ = 197.8 (*C*q), 166.3 (*C*q), 158.6 (*C*q), 158.4 (*C*q), 141.5 (*C*q), 139.8 (*C*q), 130.6 (*C*H), 129.2 (*C*q), 126.6 (*C*H), 119.6 (*C*q), 115.4 (*C*H), 114.1 (*C*H), 109.8 (*C*H), 108.8 (*C*H), 100.4 (*C*H), 66.7 (CH_2), 66.4 (CH_2), 38.3 (CH_2), 38.0 (CH_2), 27.3 (CH_3), 25.5 (*C*H), 25.0 (*C*H), 23.0 (CH_3), 22.6 ppm (CH_3) (two signals corresponding to the pyrrole α carbons were not observed due to severe exchange broadening through NH tautomerism); IR (ATR): $\tilde{\nu}$ = 3301, 2954, 2924, 2869, 1688, 1587, 1432, 1355, 1295, 1274, 1166, 1126, 1060, 1007, 981, 799, 727 cm^{-1}; UV/Vis (toluene): λ_{max} (Logε) = 408 (5.66), 491 (3.74), 521 (4.29), 558 (4.16), 600 (3.78), 658 nm (3.93); HRMS(APCI): *m/z* calcd for $C_{120}H_{133}N_8O_{14}$: 1910.9968 ([M+H]$^+$), found 1910.9968; elemental analysis calcd (%) for $C_{120}H_{132}N_8O_{14}\cdot H_2O$: C, 74.74; H, 7.00; N, 5.81; found: C, 74.75; H, 6.91; N, 5.78.

Bis-(2,7-naphthylenedioxy)-bridged porphyrin dimer 8

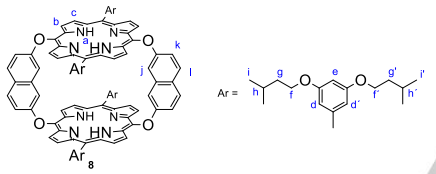

8

5,15-Dibromo-10,20-bis[3,5-bis(3-methylbutoxy)phenyl]porphyrin (**6**) (289.7 mg, 0.300 mmol), 2,7-dihydroxynaphthalene (**4**) (62.7 mg, 0.391 mmol), and K_2CO_3 (143.27 mg, 1.03 mmol) were mixed in dry DMF (45 mL). The mixture was purged with N_2 and stirred at 80 °C for 13 h, and then at 120 °C for 7 h while protected against exposure to light. The reaction mixture was diluted with $CHCl_3$, washed with water (5 × 100 mL), dried over Na_2SO_4, and concentrated under reduced pressure. The crude product was purified by flash column chromatography (silica gel, hexane/toluene 1:1), and then recrystallized from $CHCl_3$/MeOH to give **8** as a purple solid (199.1 mg, 0.103 mmol, 69%). Analytically pure sample was obtained by recrystallization from hot EtOAc as a purple powder. R_f = 0.30 (hexane : toluene = 1:1); m.p.: >300 ºC; ^{1}H NMR (500 MHz, $CDCl_3$) δ = 8.94 (d, J = 4.6 Hz, 8H, H_b), 8.58 (d, J = 4.6 Hz, 8H, H_c), 8.03 (d, J = 9.3 Hz, 4H, H_l), 7.92 (dd, J = 9.2, 2.0 Hz, 4H, H_k), 7.09 (s, 4H, H_d), 6.87 (s, 4H, $H_{d'}$), 6.75 (s, 4H, H_e), 4.54 (d, J = 2.1 Hz, 4H, H_j), 3.99 (t, J = 6.1 Hz, 16H, H_f and $H_{f'}$), 1.88–1.71 (m, 16H, H_h, $H_{h'}$, and H_g), 1.65 (q, J = 6.7 Hz, 8H, H_g), 1.01 (d, J = 6.6 Hz, 24H, H_i), 0.89 (d, J = 6.6 Hz, 24H, $H_{i'}$), −3.10 ppm (s, 4H, H_a); ^{13}C NMR (125 MHz, $CDCl_3$) δ = 164.9 (*C*q), 158.7 (*C*q), 158.3 (*C*q), 142.3 (*C*q), 134.9 (*C*q), 131.1 (*C*H), 130.4 (*C*q), 129.4 (*C*H), 127.1 (*C*H), 124.7 (*C*q), 119.9 (*C*q), 116.3 (*C*H), 114.8 (*C*H), 113.7 (*C*H), 111.4 (*C*H), 101.1 (*C*H), 66.7 (CH_2), 66.6 (CH_2), 38.1 (CH_2), 38.0 (CH_2), 25.2 (*C*H), 25.0 (*C*H), 22.9 (CH_3), 22.6 ppm (CH_3) (two signals corresponding to the pyrrole α carbons were not observed due to severe exchange broadening through NH tautomerism); IR (ATR): $\tilde{\nu}$ = 3287, 2952, 2868, 1804, 1737, 1629, 1586, 1511, 1453, 1431, 1358, 1330, 1293, 1245, 1203, 1162, 1057, 1011, 984, 957, 920, 871, 829, 792, 717 cm^{-1}; UV/Vis (toluene): λ_{max} (Logε) = 421 (5.80), 489 (3.81), 520 (4.45), 557(4.22), 599 (3.89), 657 nm (3.98); HRMS(APCI): *m/z* calcd for $C_{124}H_{133}N_8O_{12}$: 1927.0070 ([M+H]$^+$), found 1927.0089; elemental analysis calcd (%) for $C_{124}H_{132}N_8O_{12}$: C, 77.31; H, 6.91; N, 5.82; found: C, 76.95; H, 6.87; N, 5.69.

X-Ray crystal structure determinations

Purple crystals of **1b** were grown by the slow diffusion of methanol vapor into a toluene solution of **1b**. Purple crystals of **5** were grown by the slow diffusion of hexane vapor into a 4-chlorotoluene solution of **5**. Purple crystals of **7** were grown by the slow diffusion of hexane vapor into a toluene solution of **7**. Purple crystals of **8** were grown by the slow diffusion of methanol vapor into a THF solution of **8**. Single-crystal X-ray diffraction data were collected on a Rigaku XtaLab P200 diffractometer using graphite-monochromated Cu Kα radiation (λ = 1.54178 Å) for **1b** and **5**, a Bruker Smart APEX CCD diffractometer using graphite-monochromated Mo Kα radiation (λ = 0.71073 Å) for **7**, and a Rigaku XtaLab P200 diffractometer using graphite-monochromated Mo Kα radiation (λ = 0.71075 Å) for **8**. The structures were solved using SHELXS or SHELXT[21] programs and refined by full-matrix least-squares calculations on F^2 (SHELXL).[22] All non-hydrogen atoms were modeled anisotropically. Hydrogen atoms were fixed at calculated positions and refined with a riding model. In the crystal of **8**, solvent molecules were heavily disordered, and thus they were removed from the structure (and the corresponding F_0) with the SQUEEZE procedure implemented in the PLATON program suite.[23] Fourier (|*F*o|) and difference Fourier (|*F*o|−|*F*c|) maps were drawn using the ShelXle program.[24] The crystallographic data are summarized in Tables S1. For **1b** and **5**, we were not able to obtain sufficient data because of the very weak diffraction. Therefore, those data are treated as preliminary results. CCDC 1959547 (**7**), and 1970724 (**8**) contain the supplementary crystallographic data for this paper. These data can be obtained free of charge via www.ccdc.cam.ac.uk/data_request/cif.

Acknowledgements

This work was partially supported by JSPS KAKENHI Grant Numbers JP17K14447 and JP25110002.

Keywords: Aromatic substitution • Host-guest systems • Pi interactions • Porphyrinoids • Rigid dimers

[1] S. Durot, J. Taesch, V. Heitz, *Chem. Rev.* **2014**, *114*, 8542–8578.

[2] a) A. Satake, Y. Kobuke, *Org. Biomol. Chem.* **2007**, *5*, 1679; b) D. Harvey, C. Stern, C. P. Gros, R. Guilard, *Coord. Chem. Rev.* **2007**, *251*, 401–428; c) F. Bolze, C. P. Gros, M. Drouin, E. Espinosa, P. D. Harvey, R. Guilard, *J. Organomet. Chem.* **2002**, *643*, 89–97; d) S. Faure, C. Stern, R. Guilard, P. D. Harvey, *J. Am. Chem. Soc.* **2004**, *126*, 1253–1261; e) P. D. Harvey, C. Stern, C. P. Gros, R. Guilard, *J. Porphyrins Phthalocyanines* **2010**, *14*, 55–63; f) J.-M. Camus, S. M. Aly, C. Stern, R. Guilard, P. D. Harvey, *Chem. Commun.* **2011**, *47*, 8817; g) J.-M. Camus, A. Langlois, S. M. Aly, R. Guilard, P. D. Harvey, *Chem. Commun.* **2013**, *49*, 2228; h) A. Langlois, J. M. Camus, P. L. Karsenti, R. Guilard, P. D. Harvey, *Inorg. Chem.* **2017**, *56*, 2506–2517.

[3] a) A. Langlois, J. M. Camus, P. L. Karsenti, R. Guilard, P. D. Harvey, *Inorg. Chem.* **2017**, *56*, 2506–2517; b) T. Guchhait, S. Sasmal, F. S. T. Khan, S. P. Rath, *Coord. Chem. Rev.* **2017**, *337*, 112–144; c) D. Lai, F. S. T. Khan, S. P. Rath, *Dalton Trans.* **2018**, *47*, 14388–14401.

[4] a) S. K. Ghosh, R. Patra, S. P. Rath, *Inorg. Chem.* **2010**, *49*, 3449–3460; b) D. Sil, F. S. Tuglak Khan, S. P. Rath, *Inorg. Chem.* **2014**, *53*, 11925–11936; c) F. S. T. Khan, S. Banerjee, D. Kumar, S. P. Rath, *Inorg. Chem.* **2018**, *57*, 11498–11510.

[5] a) J. P. Collman, P. S. Wagenknecht, J. E. Hutchison, *Angew. Chem. Int. Ed. Engl.* **1994**, *33*, 1537–1554; b) J. Rosenthal, D. G. Nocera, *Acc. Chem. Res.* **2007**, *40*, 543–553; c) C. J. Chang, E. A. Baker, B. J. Pistorio, Y. Deng, Z. H. Loh, S. E. Miller, S. D; d) Carpenter, D. G. Nocera, *Inorg. Chem.* **2002**, *41*, 3102–3109; e) B. J. Pistorio, C. J. Chang, D. G. Nocera, *J. Am. Chem. Soc.* **2002**,

124, 7884–7885; f) J. Rosenthal, T. D. Luckett, J. M. Hodgkiss, D. G. Nocera, *J. Am. Chem. Soc.* **2006**, *128*, 6546–6547; g) Y. Le Mest, C. Inisan, A. Laouénan, M. L'Her, J. Talarmin, M. El Khalifa, J.-Y. Saillard, *J. Am. Chem. Soc.* **1997**, *119*, 6095–6106; h) S. Fukuzumi, K. Okamoto, C. P. Gros, R. Guilard, *J. Am. Chem. Soc.* **2004**, *126*, 10441–10449; i) C. J. Chang, Z. H. Loh, C. Shi, F. C. Anson, D. G. Nocera, *J. Am. Chem. Soc.* **2004**, *126*, 10013–10020; j) P. Peljo, L. Murtomäki, T. Kallio, H. J. Xu, M. Meyer, C. P. Gros, J. M. Barbe, H. H. Girault, K. Laasonen, K. Kontturi, *J. Am. Chem. Soc.* **2012**, *134*, 5974–5984.

[6] V. Valderrey, G. Aragay, P. Ballester, *Coord. Chem. Rev.* **2014**, *258–259*, 137–156.

[7] a) V. V. Borovkov, J. M. Lintuluoto, H. Sugeta, M. Fujiki, R. Arakawa, Y. Inoue, *J. Am. Chem. Soc.* **2002**, *124*, 2993–3006; b) S. Brahma, S. Asif Ikbal, S. P. Rath, *Inorganica Chim. Acta* **2011**, *372*, 62–70; c) P. Mondal, S. P. Rath, *Chem. - Asian J.* **2017**, *12*, 1824–1835; d) P. Mondal, S. Sarkar, S. P. Rath, *Chem. - Eur. J.* **2017**, *23*, 7093–7103; e) B. Saha, A. G. Petrovic, A. Dhamija, N. Berova, S. P. Rath, *Inorg. Chem.* **2019**, *58*, 11420–11438; f) R. Djemili, L. Kocher, S. Durot, A. Peuronen, K. Rissanen, V. Heitz, *Chem. - Eur. J.* **2019**, *25*, 1481–1487; g) D. Sil, F. S. T. Khan, S. P. Rath, *Chem. - Eur. J.* **2016**, *22*, 14585–14597.

[8] a) H. Lu, N. Kobayashi, *Chem. Rev.* **2016**, *116*, 6184–6261; b) S. Brahma, S. A. Ikbal, A. Dhamija, S. P. Rath, *Inorg. Chem.* **2014**, *53*, 2381–2395; c) M. Anyika, H. Gholami, K. D. Ashtekar, R. Acho, B. Borhan, *J. Am. Chem. Soc.* **2014**, *136*, 550–553; d) S. Hayashi, M. Yotsukura, M. Noji, T. Takanami, *Chem. Commun.* **2015**, *51*, 11068–11071.

[9] a) J. P. Coliman, A. O. Chong, G. B. Jameson, R. T. Oakley, E. Rose, E. R. Schmittou, J. A. Ibers, *J. Am. Chem. Soc.* **1981**, *103*, 516–533; b) C. K. Chang, I. Abdalmuhdi, *J. Org. Chem.* **1983**, *48*, 5388–5390; c) H. A. Staab, T. Carell, *Angew. Chem. Int. Ed. Engl.* **1994**, *33*, 1466–1468; d) C. J. Chang, Y. Deng, A. F. Heyduk, C. K. Chang, D. G. Nocera, *Inorg. Chem.* **2000**, *39*, 959–966; e) C. J. Chang, Y. Deng, S. M. Peng, G. H. Lee, C. Y. Yeh, D. G. Nocera, *Inorg. Chem.* **2002**, *41*, 3008–3016; f) J.-M. Barbe, C. Stern, E. Pacholska, E. Espinosa, R. Guilard, *J. Porphyrins Phthalocyanines* **2004**, *08*, 301–312.

[10] L. L. Chng, C. J. Chang, D. G. Nocera, *J. Org. Chem.* **2007**, *68*, 4075–4078.

[11] a) C. G. Oliveri, N. C. Gianneschi, S. T. Nguyen, C. a Mirkin, C. L. Stern, Z. Wawrzak, M. Pink, *J. Am. Chem. Soc.* **2006**, *128*, 16286–16296; Y. Yamada, N. Mihara, S. Shibano, K. Sugimoto, K. Tanaka, *J. Am. Chem. Soc.* **2013**, *135*, 11505–11508; c) T. Nakamura, H. Ube, M. Shionoya, *Angew. Chem.* **2013**, *125*, 12318–12322; *Angew. Chem. Int. Ed.* **2013**, *52*, 12096–12100; d) A. N. Oldacre, A. E. Friedman, T. R. Cook, *J. Am. Chem. Soc.* **2017**, *139*, 1424–1427; e) M. Kimura, J. Miyashita, S. Miyagawa, T. Kawasaki, H. Takaya, Y. Tokunaga, *Asian J. Org. Chem.* **2018**, *7*, 2087–2093; f) C. Rose, A. Lebrun, S. Clément, S. Richeter, *Chem. Commun.* **2018**, *54*, 9603–9606; g) C. Fuertes-Espinosa, A. Gómez-Torres, R. Morales-Martínez, A. Rodríguez-Fortea, C. García-Simón, F. Gándara, I. Imaz, J. Juanhuix, D. Maspoch, J. M. Poblet, L. Echegoyen, X. Ribas, *Angew. Chem.* **2018**, *130*, 11464–11469; *Angew. Chem. Int. Ed.* **2018**, *57*, 11294–11299; h) C. García-Simón, A. Monferrer, M. Garcia-Borràs, I. Imaz, D. Maspoch, M. Costas, X. Ribas, *Chem. Commun.* **2019**, *55*, 798–801.

[12] a) K. Yamashita, K. Kataoka, M. S. Asano, K. Sugiura, *Org. Lett.* **2012**, *14*, 190–193; b) K. Yamashita, S. Sakamoto, A. Suzuki, K. Sugiura, *Chem. - Asian J.* **2016**, *11*, 1004–1007; c) K. Yamashita, K. Kataoka, S. Takeuchi, K. Sugiura, *J. Org. Chem.* **2016**, *81*, 11176–11184; d) K. Yamashita, K. Kataoka, H. Pham Qui Van, T. Ogawa, K. Sugiura, *Asian J. Org. Chem.* **2018**, *7*, 2468–2478.

[13] a) L. C. Gong, D. Dolphin, *Can. J. Chem.* **1985**, *63*, 406–411; b) M. J. Crossley, L. G. King, S. M. Pyke, *Tetrahedron* **1987**, *43*, 4569–4577; c) M. J. Crossley, L. G. King, S. M. Pyke, C. W. Tansey, *J. Porphyrins Phthalocyanines* **2002**, *06*, 685–694; d) M. C. Balaban, C. Chappaz-Gillot, G. Canard, O. Fuhr, C. Roussel, T. S. Balaban, *Tetrahedron* **2009**, *65*, 3733–3739; e) A. A. Ryan, S. Plunkett, A. Casey, T. McCabe, M. O. Senge, *Chem. Commun.* **2014**, *50*, 353–355; f) C. H. Devillers, S. Hebié, D. Lucas, H. Cattey, S. Clément, S. Richeter, *J. Org. Chem.* **2014**, *79*, 6424–6434; g) Q. Chen, Y.-Z. Zhu, Q.-J. Fan, S.-C. Zhang, J.-Y. Zheng, *Org. Lett.* **2014**, *16*, 1590–1593; h) K. P. Birin, Y. G. Gorbunova, A. Y. Tsivadze, A. G. Bessmertnykh-Lemeune, R. Guilard, *Eur. J. Org. Chem.* **2015**, *2015*, 5610–5619; i) M. Kielmann, K. J. Flanagan, K. Norvaiša, D. Intrieri, M. O. Senge, *J. Org. Chem.* **2017**, *82*, 5122–5134.

[14] a) D. P. Arnold, R. C. Bott, H. Eldridge, F. M. Elms, G. Smith, M. Zojaji, *Aust. J. Chem.* **1997**, *50*, 495; b) D. E. Chumakov, A. V. Khoroshutin, A. V. Anisimov, K. I. Kobrakov, *Chem. Heterocycl. Compd.* **2009**, *45*, 259–283.

[15] SDBSWeb : https://sdbs.db.aist.go.jp (National Institute of Advanced Industrial Science and Technology, 2019)

[16] M. Kasha, H. R. Rawls, M. Ashraf El-Bayoumi, *Pure Appl. Chem.* **1965**, *11*, 371–392.

[17] a) K. Nakamura, T. Fujimoto, S. Takara, K. Sugiura, H. Miyasaka, T. Ishii, M. Yamashita, Y. Sakata, *Chem. Lett.* **2003**, *32*, 694–695; b) A. Kato, R. D. Hartnell, M. Yamashita, H. Miyasaka, K. Sugiura, D. P. Arnold, *J. Porphyrins Phthalocyanines* **2004**, *8*, 1222–1227.

[18] P. G. Seybold, M. Gouterman, *J. Mol. Spectrosc.* **1969**, *31*, 1–13.

[19] T. Funatsu, R. Iriye, H. Takai, M. Hirota, *Agric. Biol. Chem.* **1989**, *53*, 3087–3089.

[20] P. Liu, X. Xu, L. Chen, L. Ma, X. Shen, L. Hu, *Bioorg. Med. Chem.* **2014**, *22*, 1596–1607.

[21] G. M. Sheldrick, *Acta Crystallogr. Sect. A Found. Adv.* **2015**, *71*, 3–8.

[22] G. M. Sheldrick, *Acta Crystallogr. Sect. C Struct. Chem.* **2015**, *71*, 3–8.

[23] A. L. Spek, *Acta Crystallogr. Sect. C Struct. Chem.* **2015**, *71*, 9–18.

[24] C. B. Hübschle, G. M. Sheldrick, B. Dittrich, *J. Appl. Crystallogr.* **2011**, *44*, 1281–1284.

10.1002/cplu.201900670

WILEY-VCH

Entry for the Table of Contents (Please choose one layout)

Layout 1:

FULL PAPER

A series of porphyrin dimers bridged by one or two arylenedioxy linkers was successfully synthesized in high yields by catalyst-free nucleophilic aromatic substitution. The orientational freedom and conformation of the two porphyrin macrocycles in the mono-bridged dimers were controlled by the substituents on the arylenedioxy linkers. Bis-bridged dimers exhibited a highly rigid cofacial conformation.

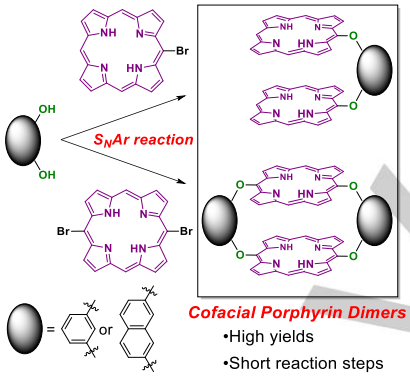

Ken-ichi Yamashita, Narumi Kuramochi, Hang Pham Qui Van, Kazuhiro Furutani, Takuji Ogawa, Ken-ichi Sugiura**

Page No. – Page No.

Efficient Synthesis of Arylenedioxy-Bridged Porphyrin Dimers through Catalyst-Free Nucleophilic Aromatic Substitution